ORIGINAL RESEARCH
https://doi.org/10.4209/aaqr.210398

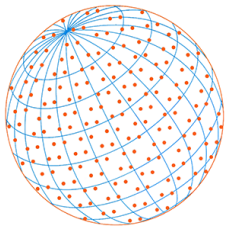

Aerosol and Air Quality Research

Special Issue:
Air Pollution and its Impact in South and Southeast Asia (II)

Retrieval of NO_2 Columns by Exploiting MAX-DOAS Observations and Comparison with OMI and TROPOMI Data during the Time Period of 2015–2019

Ahmad Iqbal[1], Naveed Ahmad[1], Hassan Mohy ud Din[1], Michel Van Roozendael[2], Muhammad Shehzaib Anjum[1], Muhammad Zeeshan Ali Khan[1], Muhammad Fahim Khokhar[1*]

[1] Institute of Environmental Science and Engineering (IESE), National University of Science and Technology (NUST), Islamabad-44000, Pakistan
[2] Royal Belgian Institute for Space Aeronomy (B), Brussels, Belgium

ABSTRACT

Nitrogen dioxide (NO_2)—a criteria major air pollutant, is of paramount importance due to its role in atmospheric chemistry and tropospheric ozone formation. Exposure to high concentrations of NO_2 has been reported to cause various health issues in humans. This study presents an intercomparison of NO_2 retrieval settings using the Differential Optical Absorption Spectroscopy (DOAS) and based on the literature published over the last 20 years. Comparison between results of various settings, as reported in the literature, and settings used for this study show a good correlation with $R^2 > 0.97$. This paper also presents validation of satellite observation through ground-based MAX-DOAS measurements from September 2015 to September 2019. Daily MAX-DOAS measurements have shown a strong positive correlation of 70.75% and 77.74% with OMI and TROPOMI, respectively. The average monthly correlation for OMI and TROPOMI with MAX-DOAS is 88.39% and 91.91% respectively. The comparison of the slopes of regression plots for daily and monthly datasets of OMI and TROPOMI vs. MAX-DOAS reveals that TROPOMI data is more synonymous to MAX-DOAS than OMI data. The error analysis indicates that for TROPOMI measurements calculated biases are significantly improved in case of TROPOMI as compared to OMI measurements. It is pertinent to mention that TROPOMI measurements can capture the local NO_2 pollution much better than OMI and its predecessor instruments like GOME-2, SCIAMACHY and GOME. Seasonal trends of NO_2 column densities have shown a peak in the winter season (November–January) while lowest NO_2 column density is recorded in monsoon season.

Keywords: NO_2 retrieval settings, DOAS Algorithm, Satellite observations, Validations

Received: December 28, 2021
Revised: April 22, 2022
Accepted: April 30, 2022

* **Corresponding Author:**
fahim.khokhar@iese.nust.edu.pk

Publisher:
Taiwan Association for Aerosol Research
ISSN: 1680-8584 print
ISSN: 2071-1409 online

1 INTRODUCTION

Nitrogen dioxide (NO_2) is of prime importance due to its active role in the photochemistry of the atmosphere (Ma *et al.*, 2013; Chan *et al.*, 2015). NO_2 is also one of the major criteria air pollutants, which poses serious threats to human health (WHO, 2006).

Exposure to high concentrations of nitrogen dioxide has been reported to cause damage to the respiratory system and aggravates bronchitis in some cases (Valavanidis *et al.*, 2008; Ma *et al.*, 2013; Khokhar *et al.*, 2017). Furthermore, exposure to NO_2 has been considered the root cause of reduced lungs efficiency in infants (Trasande and Thurston, 2005) and exacerbating asthma among primary school children (Youssef Agha *et al.*, 2012). However, higher incidents of lung diseases have been associated with long-term exposure to NO_2 (Soto-Martinez and Sly, 2010). Especially in developing countries like Pakistan, lack of political will, inadequate resources, and

air quality monitoring infrastructure combined with weak enforcement of air pollution standards have primarily increased the vulnerability of humans to air pollution-related diseases (Ali *et al.*, 2021; Anjum *et al.*, 2021).

The importance of nitrogen dioxide in the atmosphere is not only due to its health effects but also because (a) it absorbs solar radiation and reduces atmospheric visibility (Majewski *et al.*, 2014); (b) it affects the oxidizing capacity of the troposphere by reacting with radical species, like hydroxyl radical, present in the atmosphere, (c) it plays a crucial role in maintaining ozone concentration in the troposphere as it initiates the catalytic formation of ozone (U.S. EPA, 2006).

Sources of NO_2 include both natural and anthropogenic activities. But most of these sources are related to the burning of biomass, fossil fuel consumption, and different industrial emissions (Tack *et al.*, 2015; Gratsea *et al.*, 2016; Chan, 2017; Malik *et al.*, 2020). On the other hand, it is mainly removed from the atmosphere through its reaction with free radicals like hydroxyl radicals (OH) and ozone (O_3), which ultimately results in Nitric acid and NO_3 (Crutzen, 1970; Athanasopoulou *et al.*, 2008; Wang *et al.*, 2012; Yang *et al.*, 2019).

In recent years, optical methods were used to perform NO_2 measurements in the atmosphere. The advantages of this method are high sensitivity, fast measurements and simultaneous detection of several trace gases (Lohberger *et al.*, 2004). In particular, multi-axis DOAS (MAX-DOAS) instruments (Hönninger *et al.*, 2004; Platt and Stutz, 2008; Vlemmix *et al.*, 2015) have been used for the retrieval of vertical column densities of various tropospheric trace gases (NO_2, O_3, CHOCHO, SO_2, BRO, IO, HCHO and HONO) (Leser *et al.*, 2003; Coburn *et al.*, 2011; Hendrick *et al.*, 2014; Wang *et al.*, 2017; Khan *et al.*, 2018; Chan *et al.*, 2019; Kreher *et al.*, 2019; Javed *et al.*, 2019a, b). MAX-DOAS measurements can be performed from different platforms like ground-based, vehicle-based, ship-based and satellite-based (Halla *et al.*, 2011; Peters *et al.*, 2012; Lin *et al.*, 2014; Shaiganfar *et al.*, 2015; Dix *et al.*, 2016; Shabbir *et al.*, 2016). Cheng *et al.* (2019) explored the temporal variation of tropospheric NO_2 vertical column densities (VCDs) using MAX-DOAS measurements in Shangdianzi region of China and compared them with OMI data. In another study, MAX-DOAS has been used for the observation of tropospheric SO_2, NO_2, and HCHO in Hefei, Nanjing, and Shanghai (Yangtze River Delta area) (Tian *et al.*, 2018). Longer-term studies covering more than 5 years were also conducted using Max-DOAS (Chan *et al.*, 2018).

In Pakistan, air pollution is a predictable key environmental issue as it is ranked in the top polluted countries in the region. The recurrence of smog episodes in Pakistan and neighboring regions is a clear manifestation of worsened air quality and consequent disruption in socio-economic circles (Khokhar *et al.*, 2021; Anwar *et al.*, 2021). The menace of degraded air quality is aided by economic development, unprecedented increase in the vehicular fleet, poor quality of fuel, and lack of any satisfactory measures due to the absence of a proper air quality monitoring network. Large-scale mitigation measures are direly needed to be taken to maintain ambient air quality within permissible limits. Very few studies have been conducted in Pakistan to measure the atmospheric levels of NO_2 in Pakistan (Ali and Athar, 2008; Tariq *et al.*, 2014; Khokhar *et al.*, 2016b; Zeb *et al.*, 2019; Bilal *et al.*, 2021). For instance, Zeb *et al.* (2019) exploited multiple satellite instruments to identify the spatial and decadal variation of trace gases in Pakistan. In a similar study, Shabbir *et al.* (2016) have used Car-mounted MAX-DOAS to measure the NO_2 concentration over the NH5 highway from Islamabad to Lahore, in Pakistan. However, so far, no validation has been performed in the moderately polluted city of Islamabad, where temporal gradients of NO_2 are small.

Thus, the objective of this study is to present (a) the assessment of a DOAS fit NO_2 retrieval suitable for measurements at Islamabad (b) an intercomparison between a large number of NO_2 DOAS retrieval settings consistently applied to the same spectral data, and (c) the use of ground-based tropospheric NO_2 measurements performed at Islamabad to validate satellite observations from the OMI and TROPOMI instruments.

This paper is organized as follows In Section 2, the design of the intercomparison study is discussed including the instrument, study site, and measurement protocol. In Section 3, results of a regression analysis of various NO_2 retrieval settings are presented. In Section 4, the validation of OMI and TROPOMI satellite observations using ground-based MAX-DOAS data are discussed. Finally, Section 5 provides a conclusion of the study.

ORIGINAL RESEARCH
https://doi.org/10.4209/aaqr.210398

2 DESIGN OF INTERCOMPARISON STUDY AND MEASUREMENT PROTOCOL

2.1 Introduction

Various studies have been conducted previously for the retrieval of NO_2 measurements by the MAX-DOAS technique. In this study, settings extracted from the literature were used to conduct an intercomparison of DOAS fit settings performed on data recorded on 1 November 2017. We used results from this exercise, to define optimal settings for NO_2 measurements at Islamabad, Pakistan. Table S1 contains a list of the settings that were used for DOAS analysis on 1 November 2017. The table lists the studies included, Wavelength ranges for each study, and absorber fitted used in a specific study. It also includes various parameters retrieved e.g., Maximum dSCD (molecules cm^{-2}), Average dSCD (molecules cm^{-2}), RMS, spectrum shift and dSCD error (molecules cm^{-2}).

2.2 Differential Optical Absorption Spectrometry (DOAS) Technique

The DOAS technique used in this study is based on the Lambert-Beer law which states that the transmittance of light through an absorbing medium is directly proportional to the concentration of the substance present in the optical path.

$$I(\lambda) = Io(\lambda)e - \alpha LC \quad (1)$$

Here, in Eq. (1) "Io" means incident intensity whereas "I" is referred to the measured intensity. Various trace gases can be obtained simultaneously within a selected fitting interval. The retrieval method considers laboratory absorption cross-sections and by using spectra of the desired gases, slant column densities (SCDs) can be retrieved using a linear-least squares minimization. The DOAS technique is especially used for the retrieval of trace gases that have a short lifetime in the atmosphere like NO_2.

2.3 Measurement and Data Analysis Protocol for the Development of New Retrieval Settings for NO_2

QDOAS is retrieval software designed by the Royal Belgium Institute for Space and Aeronomy for the analysis of UV-visible spectra. Different cross-sections: NO_2 at 298 K (Vandaele *et al.*, 1996), NO_2 a at 220 K (Vandaele *et al.*, 1996), O_3 at 223 K (Serdyuchenko *et al.*, 2014), O_4 at 293 K (Thalman and Volkamer, 2013), H_2O (Rothman, 2010) and Ring were used in the fitting interval of 409–445 nm for the development of the optimized NO_2 retrieval settings considered in this study (see Table S1). Measurements were carried out at elevation angles 2°, 4°, 5°, 10°, 15°, 30°, 45°, and 90° and polynomial order of 4 was selected. To minimize the stratospheric influence, the zenith spectrum of each cycle was used. The residual spectrum that remains after subtracting all absorption cross-sections through least-squares minimization is characterized by its root mean square (RMS). It is generally of the order of 10^{-4} or higher for good instruments. Different trace gases cross-sections and aerosols retrieval play important role in the uncertainty of the vertical column densities (VCDs). Sites with low trace gases can have higher uncertainty in retrieved VCDs. The uncertainties introduced by the geometric approximation depend on the viewing geometry and the aerosol load. However, instrumental conditions can also affect the uncertainty and accuracy of the results. Many studies conducted previously have revealed that typical error in VCDs retrieved by MAX-DOAS is around 20% (Hendrick *et al.*, 2014; Wang *et al.*, 2014; Franco *et al.*, 2015). Fig. 1 shows an example of a DOAS fit for NO_2. Red lines represent the reference spectrum and the black line shows the measured spectrum after subtracting all other absorbers. It was measured on 23 May 2018 at 12:36 UTC. SZA was 73° and the elevation angle was 5°. The mean dSCD value for this fit was 3.55×10^{16} molecules cm^{-2}. Differential slant column densities depend upon the light pathways which is characterized by an air mass factor (AMF) usually calculated using a radiative transfer model. In this study, however the AMF was estimated using a simple geometric approximation as described in (Hönninger *et al.*, 2004; Wittrock *et al.*, 2004; Wagner *et al.*, 2010). This method allows the retrieval of column densities of trace gases even in cloudy conditions (Wagner *et al.*, 2010).

ORIGINAL RESEARCH
https://doi.org/10.4209/aaqr.210398

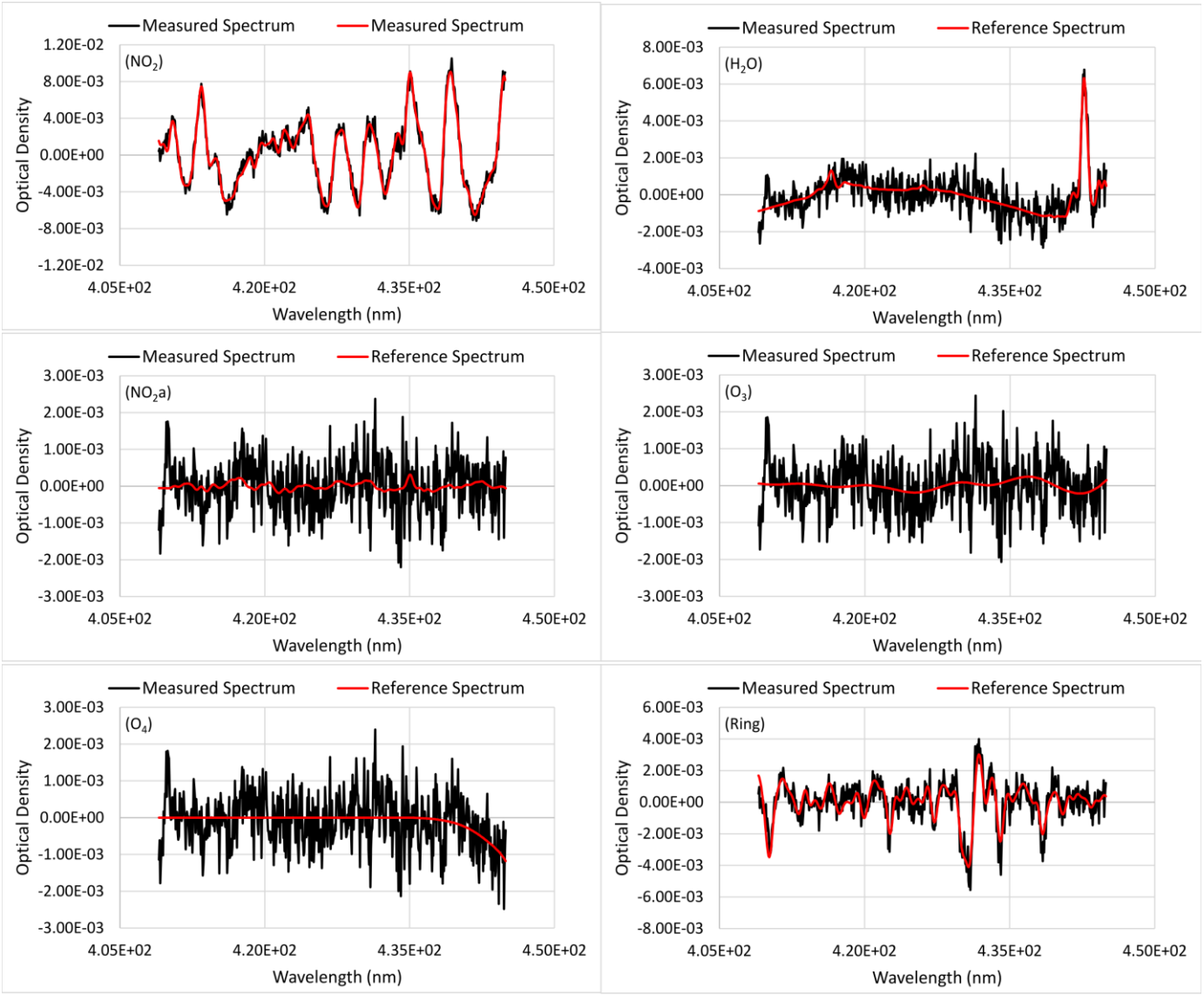

Fig. 1. The DOAS fit observed for NO_2 on 23 May 2018 at 5° elevation angle and SZA of 73°.

$$VCD = SCD/AMF \quad (2)$$

A differential air mass factor (dAMF) was used because the slant column densities obtained were differential SCDs corresponding to the difference between SCDs measured at low elevations and dSCDs recorded at the zenith for the same scan (Liu *et al.*, 2016).

$$VCDtrop = dSCD\alpha / dAMF\alpha \quad (3)$$

dAMF is difference in AMF obtained at a certain angle and AMF obtained at 90°:

$$dAMF\alpha = AMF\alpha - AMF90° \quad (4)$$

So, Eq. (3) will be:

$$VCD_{trop} = dSCD\alpha / AMF\alpha - AMF90° \quad (5)$$

Using geometric approximation, AMF can be found as:

ORIGINAL RESEARCH
https://doi.org/10.4209/aaqr.210398

$$AMF = 1/sin\alpha \quad (6)$$

Then Eq. (5) will be:

$$VCD_{trop} = dSCD\alpha \,/\, 1/sin(\alpha - 1) \quad (7)$$

This method has been used widely to derive the tropospheric vertical column (VCD) of trace gases. Despite its simplicity, it works with good accuracy for NO_2 when applied to measurements at 30° of elevation.

2.4 Instrument

To quantify the tropospheric trace gases, the MAX-DOAS uses different elevation angles, from 0 to 90°, to capture the scattered sunlight (Bobrowski *et al.*, 2003). MAX-DOAS can measure several trace gases, at a time, in the visible and Ultra-Violet Spectral ranges and the resultant less residual allows its use in even less polluted environment. The MAX-DOAS instrument used in this study is based on a light weight spectrometer with dimensions of 13 cm × 19 cm × 14 cm. It contains a 40 mm lens mounted at the front, coupled with the spectrograph by fiber optics and an electronic circuit. Czerny-Turner spectrometer (USB 2000+, Ocean Optics In.), having a spectral resolution of 0.7 nm, records the solar scattered light between 320–460 nm. A stepper motor, installed in it, is used to move the entire instrument to achieve the desired elevation angle. Scattered light enters the instrument via a lens that is tightly sealed to avoid any condensation of water vapors and prevent dust particles to damage the interior optics.

In this study, DOAS fit retrieval settings were used to analyze the MAX-DOAS measurements from September 2015 to September 2019. The OMI observations (https://disc.gsfc.nasa.gov/datasets/OMNO2d_003/summary) for this period were obtained from GIOVANNI and the data product used was "NO_2 Tropospheric column 30% cloud screened ($OMNO_2$d v003)" for better agreement of tropospheric NO_2. However, later on, the tropospheric monitoring instrument (TROPOMI) data (https://developers.google.com/earth-engine/datasets/catalog/COPERNICUS_S5P_NRTI_L3_NO_2) was also available starting from August 2018. TROPOMI product of tropospheric NO_2 column number density (having a spatial resolution of 7 × 3.5 km was taken through the Google Earth Engine platform (ee.ImageCollection("COPERNICUS/S5P/NRTI/L3_NO2")) from September 2018 to September 2019. TROPOMI is a satellite instrument onboard Sentinel 5P satellite.

Slant Column Densities obtained from OMI and their uncertainties have been affected by the instrument's degradation (radiometric), row irregularity and stripes. According to a study, temporal analysis of NO_2 Slant column Density uncertainty over the period of 2005–2016 has been $0.013 \times 10^{15} \pm 0.001 \times 10^{15}$ molec. cm^{-2} $year^{-1}$ (Zara *et al.*, 2018). Uptil now, less than 5% optical degradation in visible channel of OMI has been observed (Boersma *et al.*, 2011; Müller *et al.*, 2016; Schenkeveld *et al.*, 2017). Similarly, noise is also increasing gradually over the period of time owing to the long-term use of CCD detector (Schenkeveld *et al.*, 2017). Furthermore, the details on the slant column retrieval method, stability, uncertainties for TROPOMI NO_2 measurements and its comparison with OMI are available in a study conducted by Van Geffen *et al.* (2020).

2.5 Measurement Site

Islamabad, the capital of Pakistan was selected as a site for this study. Pakistan's climate is described by four seasons based on the occurrence of monsoon: Winter (December–February), Pre-Monsoon (March–May), Monsoon (June–September) and Post Monsoon (October–November) (Naheed *et al.*, 2013). Islamabad is located at the latitude of 33.349°N; and longitude of 72.324°E, at an elevation above sea level of 450 meters (1827 ft). Islamabad is a mountainous region located in the Pothohar Plateau. The instrument was mounted on the rooftop of the Institute of Environmental Sciences and Engineering (IESE), National University of Sciences and Technology (NUST) Islamabad, Pakistan. The lowest elevation angle used in this study was 2°.

ORIGINAL RESEARCH
https://doi.org/10.4209/aaqr.210398

3 RESULTS

3.1 Comparison of dSCD, RMS, and Slant Error Retrieved for Intercomparison of NO_2 DOAS Fit Settings Listed in Table S1

A sensitive study was constructed to find optimal settings for retrieval of NO_2 using MAX-DOAS for local climatic conditions. The efforts for this study are inspired by the QA4ECV project (http://www.qa4ecv.eu/) in which algorithms were improved for satellite NO_2 retrievals. Similarly, this study attempts to find optimum settings for NO_2 retrieval through ground-based MAX-DOAS for local conditions in Islamabad. Though sensitivity to NO_2 spectral lines is generally known to be highest in the 400–450 nm region, analysis were carried out to find the best fitting sub-window in this range that could further improve the results and reduce the RMS and Slant column error of the data obtained at the site. Moreover, different O_4 cross-sections were also analyzed to find out the most suitable one for the NO_2 retrieval in the study area. These were Thalman and Volkamer (2013) at 293 K, Hermans (2011) at 298 K, Thalman and Volkamer (2013) at 203 K and Burkholder and Talukdar (1994). Among these, Burkholder cross-section improved the O_4 best fit. Moreover, RMS and dSCDs were also improved by using Burkholder cross-section.

In addition to this, a wavelength range of 320 nm to 445 nm was used keeping in view the spectral range of an available MAX-DOAS instrument. Initially, the upper boundary of the fitting interval was kept constant at 445nm whereas the lower boundary was increased up to 420 nm with an interval of 10 nm each. Then lower boundary was kept constant at 320 nm and the upper boundary was reduced from 445nm up to 355 nm with an interval of 10 nm each. Consequently, RMS, Slant error and dSCDs of each fitting interval were compared and the least RMS and Slant error was observed at 410 nm to 445nm interval as the lower and upper boundary of fitting interval respectively. Further analysis with 409 nm–445 nm as fitting window and Burkholder O_4 cross-section for NO_2 retrieval shows reduction of RMS and NO_2 slant column error. Thus, this setting was considered as optimum for the study area i.e., Islamabad. Moreover, to compare the settings of this study, literature was consulted with studies having fitting windows within the range of fitting interval of the instrument used in this study i.e., 320 nm–465 nm. Thus, the reported settings of 19 studies (for more details, see Table S1) were used to analyze and compare the results with the settings found in this study. Fig. 2(a) shows dSCDs of NO_2 obtained at an elevation angle 10° on 1 November 2017. It can be observed that dSCDs obtained using optimal settings of this study are among the highest as compared to dSCDs obtained by using the settings of previous studies reported in the literature. dSCDs obtained using Shaiganfar *et al.* (2011) settings show the highest values but corresponding RMS are larger than those obtained using the settings of this study. The comparison of the NO_2 RMS obtained using the various settings considered for this study is shown in Fig. 2(b). It clearly shows that the RMS for dSCDs obtained by using the settings of this study is low as compared to that of most of the others. Similarly, Fig. 2(c) shows the slant column error for the NO_2 dSCDs measured in this study is among the lowest. The DOAS fit retrieval settings for NO_2 used in this study have not only reduced Slant error and RMS but also improved dSCDs which depicts that these settings are suitable for the study site.

3.2 Regression Analysis

To intercompare the different data sets, linear regressions were performed using data sets obtained with standard (optimized) settings of this study as a reference. Accordingly, dSCDs retrieved from different settings found in the literature were used to draw correlation plots as shown in Fig. 3. As can be seen, a tight correlation is observed for most of the cases. However, the highest correlation (R^2 = 0.999) is found with the settings of Drosoglou *et al.* (2018) which includes a strong NO_2 absorption band of 411–445 nm. Whereas, Lee *et al.* (2009) have shown the lowest value (R^2 = 0.972) which includes an absorption band of 364–383 nm (for more details see Table S1). It can be attributed to the wavelength dependency of tropospheric NO_2 AMFs. For instance, Lee *et al.* (2009) has used a spectral fitting window of (364–383 nm) which falls in the UV-A spectral range and identified a longer light path and higher extinction coefficient. Furthermore, it might be largely impacted by the Rayleigh scattering dominant towards a shorter wavelength. However, wavelength window 409–445nm, was used in this study for further retrieval of NO_2 dSCDs. The values for the slope, intercept and RMS are calculated as a part of the regression analysis.

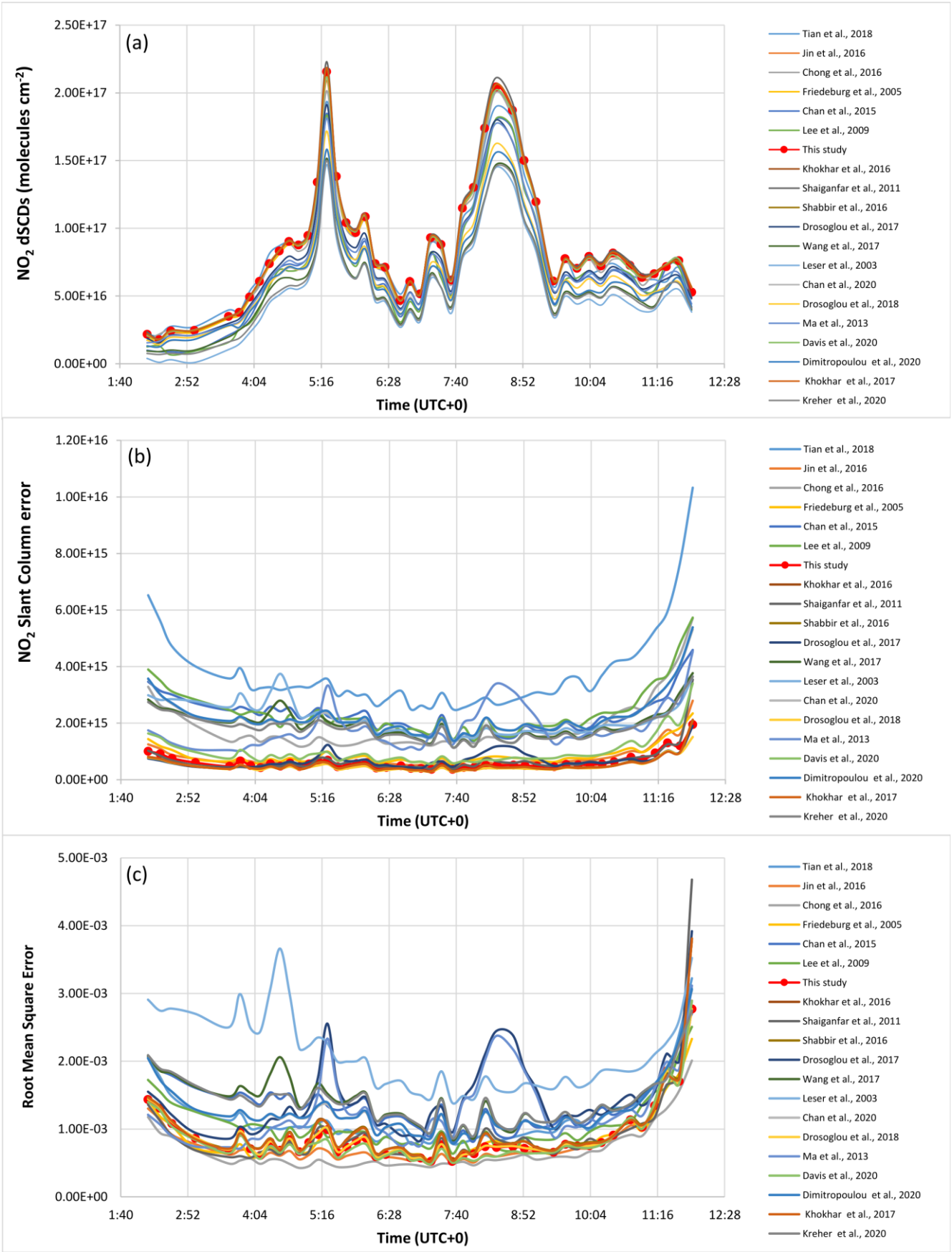

Fig. 2. Comparison of (a) NO_2 dSCDs, (b) RMS and (c) Slant Column error retrieved by MAX-DOAS through various DOAS fit settings used in literature and settings used for this study.

ORIGINAL RESEARCH
https://doi.org/10.4209/aaqr.210398

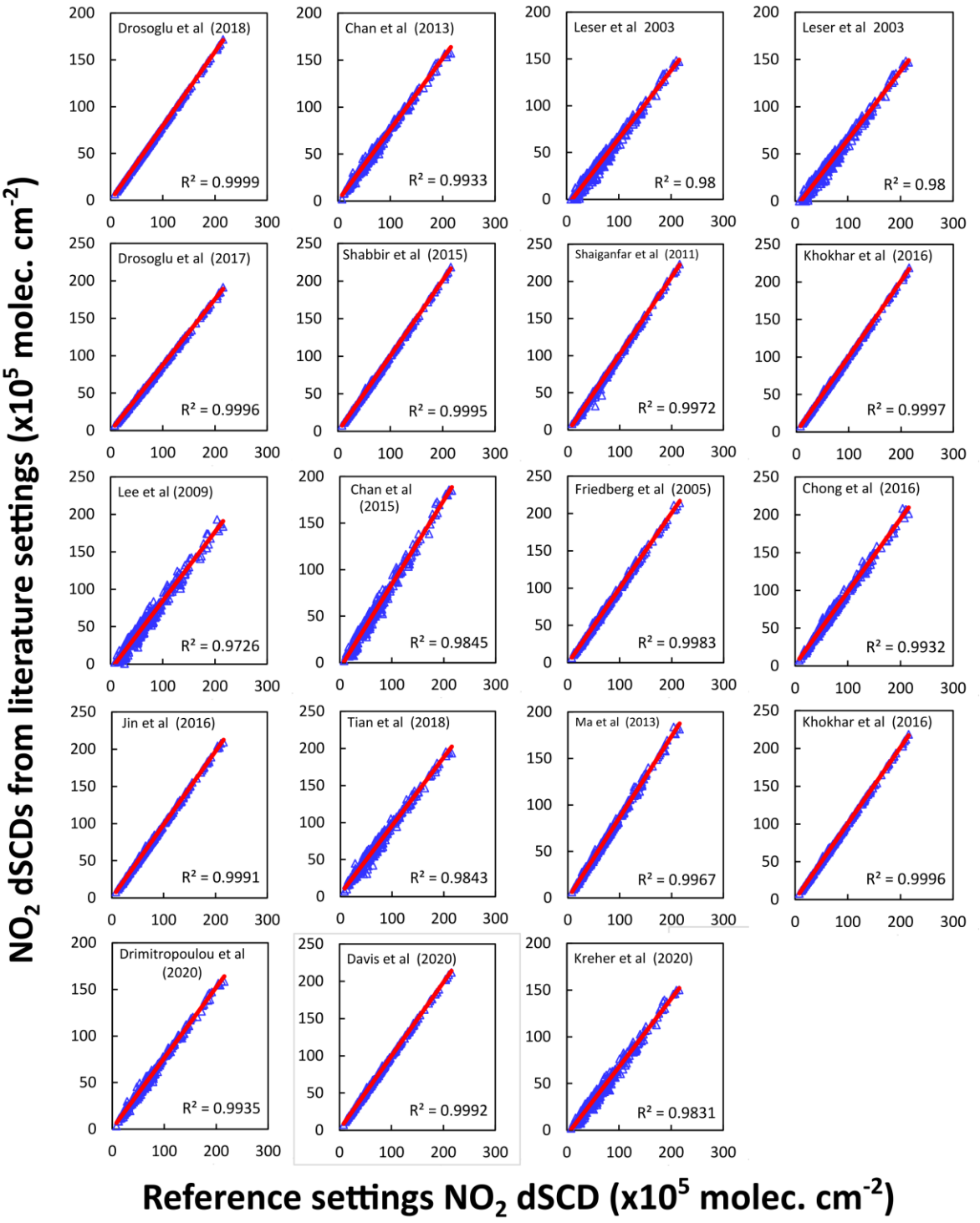

Fig. 3. Regression analysis of NO_2 dSCDs for various DOAS fit retrieval settings found in literature plotted against the reference DOAS fit retrieval settings used for this study.

Whereas, Spectrum shift is obtained from the DOAS retrieval algorithm used for MAX-DOAS data analysis. Fig. 4 presents a different view of the data set already presented in Fig. 3. It shows RMS, slope, intercept, and spectrum shift calculated from regression analysis for all the measurements obtained by different settings with settings found in this study. It was done for different elevation viewing angles (2°, 4°, 5°, 10°, 15°, 30°, and 45°). Values are colored according to the elevation viewing angles. The dash lines indicate the standard deviation for slope, intercept, and spectrum shift whereas in RMS it represents the average value. A close relation of the parameters is observed

ORIGINAL RESEARCH
https://doi.org/10.4209/aaqr.210398

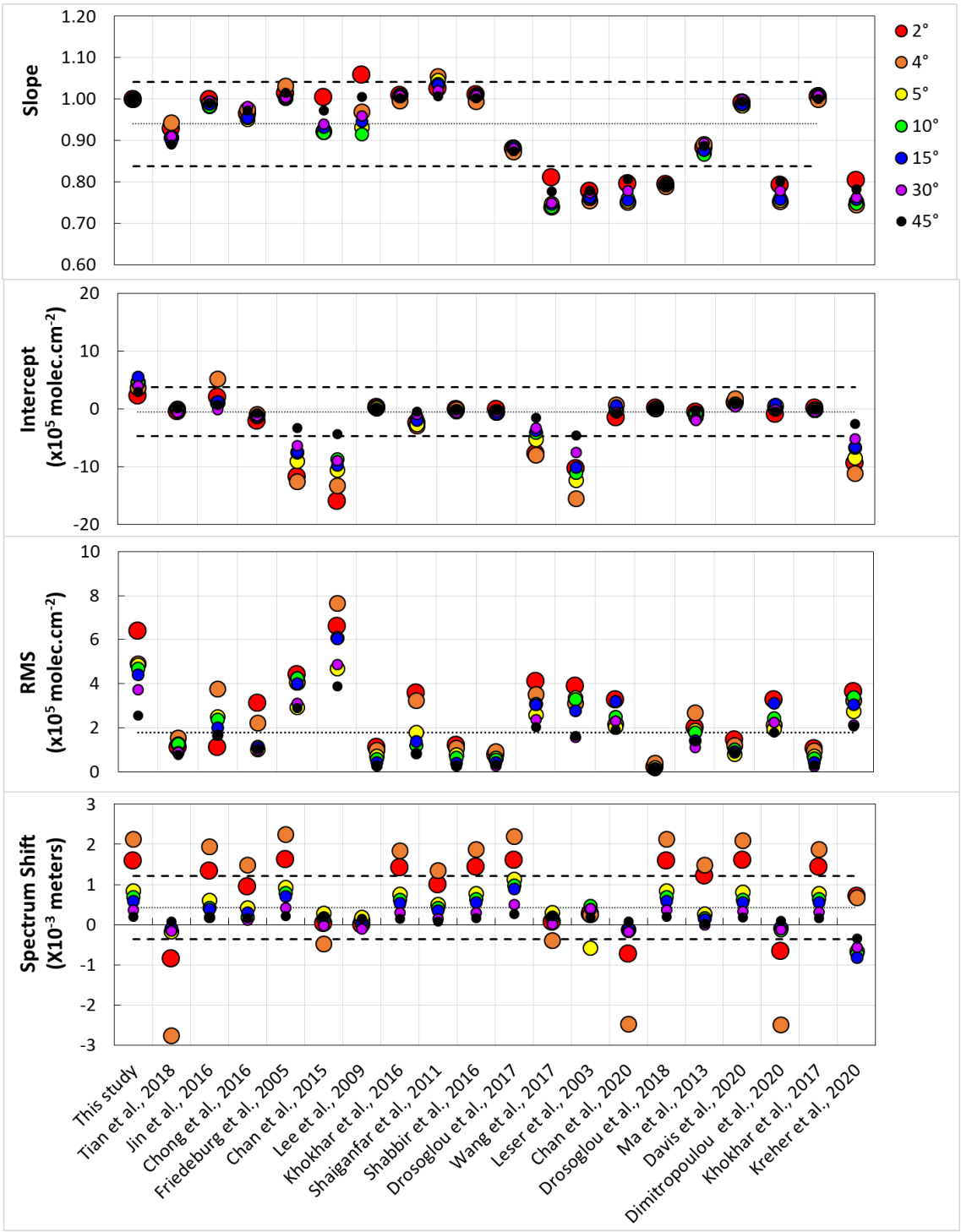

Fig. 4. Slope, intercept, spectrum shift and RMS of regression analysis for dSCDs of various DOAS fit retrieval settings found in literature plotted against the reference DOAS fit retrieval settings of this study.

among all the settings used for different elevation angles. Three parameters of regression used in Fig. 4 (RMS, slope, and intercept) do not display any significant angular dependency. Some data display larger deviations irrespective of elevation angles. For instance, RMS for Tian *et al.* (2018), Chan *et al.* (2015), and Lee *et al.* (2009) lie above the mean value. Whereas, for slope, Shaiganfar *et al.* (2011), Wang *et al.* (2017), Leser *et al.* (2003), Chan *et al.* (2020), Dimitropoulou *et al.* (2020) and Kreher *et al.* (2020) showed largest deviations. However, a larger Spectrum Shift is observed at smaller angles as shown in Fig. 4.

ORIGINAL RESEARCH
https://doi.org/10.4209/aaqr.210398

4 VALIDATION OF SATELLITE TROPOSPHERIC NO_2 OBSERVATIONS

The spatial extent and magnitude of tropospheric NO_2 columns over Islamabad are highlighted in Fig. 5. The lower two panels show the OMI obtained area-averaged maps for Islamabad. Where the bottom map represents the time periods between October 2004 to September. 2019 and the second panel represents the period between September 2018 and September 2019. A very minute difference can be seen between the two maps showing that there has been very little significant change in the spatial extent of NO_2. This could also be a result of the coarse resolution of the OMI. The first panel of Fig. 5 highlights the TROPOMI Tropospheric NO_2 columns, also for the time period September 2018 to 2019. It is apparent that the better spatial resolution (7×3.5 km^2 during the study duration for which data is used) of the TRPOMI instrument helps differentiate between hotspots more easily. In this case, the higher levels of NO_2 are observed near congested roads and densely packed areas of Islamabad city while peri-urban and rural areas in the vicinity of Islamabad are showing relatively lower NO_2 columns. However, it is important to note that there is not a stark difference between the distributions of pollution levels for the long-term averaged map and the yearly map from OMI instrument. This urges the need for comprehensive ground-based observations for the validation of satellite products that can be used for pollution management and to devise abatement strategies. Thus, this study having NO_2 columns observed by the MAX-DOAS instrument at the IESE-NUST site in combination with satellite data can serve such purposes to a certain extent. Especially, areas without having a regular air pollution monitoring network.

The comparison of available data for all three instruments i.e., ground-based, and two satellites is presented in Figs. 6(a) and 6(b). The data for ground-based MAX-DOAS and OMI was available from September 2015 to September 2019 except for January and February 2016. The data for TROPOMI was available from September 2018 to September 2019. Initially, the on-site ground-based MAX-DOAS VCDs for the study period were averaged over a local time of 1300 hrs to 1400 hrs on daily basis as the TROPOMI and OMI over passing time are 1330 hrs and 1340 hrs

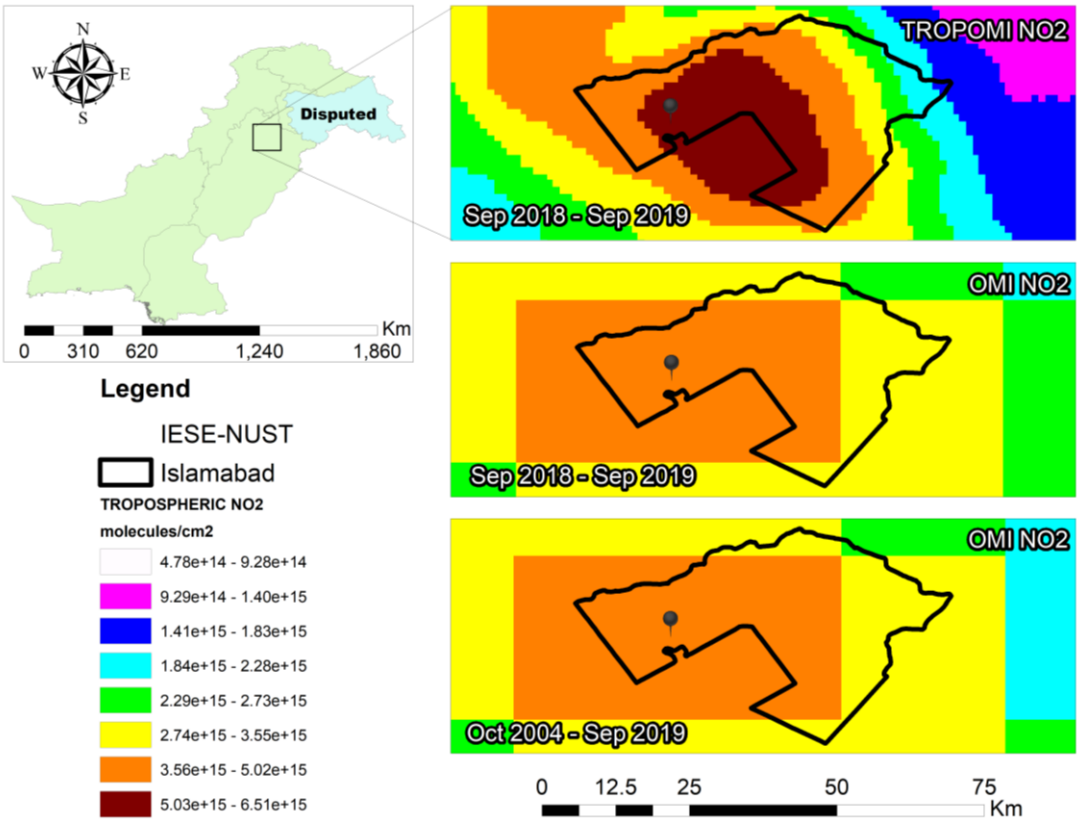

Fig. 5. Spatial and temporal extent of NO_2 columns over Islamabad using OMI and TROPOMI data.

ORIGINAL RESEARCH
https://doi.org/10.4209/aaqr.210398

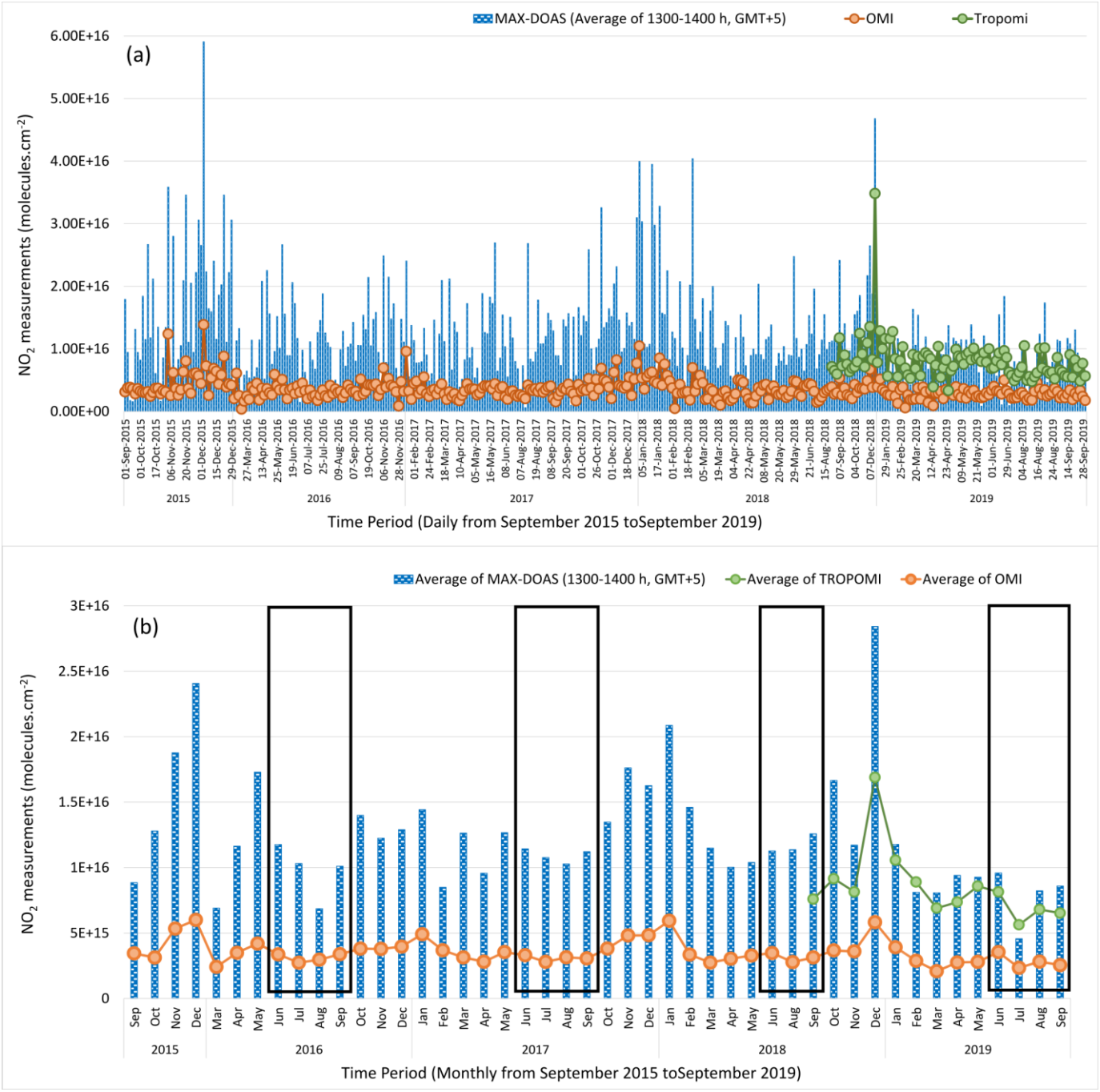

Fig. 6. Comparison of (a) daily (b) monthly vertical column densities (VCDs) retrieved through ground-based MAX-DOAS, tropospheric NO_2 column densities by OMI, and tropospheric NO_2 column densities by TROPOMI from September 2015 to September 2019. Grey rectangles in lower panel (b) indicate the monsoon period in Pakistan.

respectively. So, averaged MAX-DOAS VCDs (1300 hrs–1400 hrs local time) were used for satellite validation. Further, the data was filtered on daily basis keeping in view the cloud cover of less than 20% and to make sure the comparison of three instruments for same-day i.e., the comparison is shown for all those days for which data is available for all three instruments (see Fig. 6(a)). The comparison for daily measurements of three instruments i.e., ground-based MAX-DOAS, OMI, and TROPOMI is presented in Fig. 6(a) while the monthly comparison for these instruments is shown in Fig. 6(b). Fig. 6(a) shows that daily satellite observations (OMI and TROPOMI) are corresponding to MAX-DOAS observations and showing a similar trend for the entire period but values are lower as compared to the measurements obtained by ground-based MAX-DOAS. However, the values

ORIGINAL RESEARCH
https://doi.org/10.4209/aaqr.210398

obtained for TROPOMI are higher and showed good agreement with MAX-DOAS as compared to OMI. It is mainly because of the higher spatial resolution of TROPOMI (7 × 3.5 km^2) as compared to OMI (13 × 24 km^2) in addition to better spectral resolution i.e., 0.54 nm and 0.63 nm for TROPOMI and OMI respectively, and improved signal to noise ratio of around 1500 for TROPOMI and around 500 for OMI. Therefore, TROPOMI measurements are able to capture the local NO_2 pollution much better than OMI. However, satellite instruments quantitively underestimated NO_2 columns (see Fig. 6(a)) for the entire period as compared to ground-based MAX-DOAS amidst to the fact that satellites average over larger ground pixel sizes and are relatively less sensitive to boundary layer pollution.

Moreover, satellite observations through OMI and TROPOMI are showing the same trend as that of ground observations through MAX-DOAS (see Fig. 6(b)). Also, owing to its high spatial resolution, it is pertinent to mention that TROPOMI measurements are able to capture the local NO_2 pollution much better than OMI and its predecessor instruments like GOME-2, SCIAMACHY, GOME.

Considering the data from three instruments, linear regressions were performed for daily as well as monthly measurements of these instruments. Linear regression was performed for ground-based MAX DOAS vs. OMI and ground-based MAX-DOAS vs. TROPOMI. The correlation for daily measurements between MAX-DOAS and OMI has shown a very good positive correlation with $R^2 = 0.50$ ($r = 0.70$) as shown in Fig. 7(a). Fig. 7(b) shows a positive correlation between daily NO_2 measurements of ground-based MAX-DOAS and TROPOMI. This shows an improved correlation with $R^2 = 0.60$ ($r = 0.77$) which could be due to improved spatial resolution of TROPOMI as compared to OMI. The monthly correlation of ground-based MAX-DOAS with OMI and TROPOMI is shown in Figs. 7(c) and 7(d) respectively. It has shown a high positive correlation with $R^2 = 0.78$ ($r = 0.88$) for OMI (see Fig. 7(c)) While it also depicts an improved and high positive correlation with $R^2 = 0.84$ ($r = 0.91$) for TROPOMI (see Fig. 7(d)). Through linear regression and correlation plots, it can be seen that the instruments i.e., ground-based MAX-DOAS vs. OMI and ground-based MAX-DOAS vs. TROPOMI have shown a strong positive correlation for daily as well as for monthly NO_2 measurements.

The slope of the regression analysis between MAX-DOAS and TROPOMI depicts a linear positive relationship between the two (see Fig. 7(b)). The value of slope for this model is 0.1893 for TROPOMI. The slope value shows underestimation by TROPOMI as the slope is nearer to 0 than 1 (i.e., 0.1). On the other hand, values obtained from the OMI satellite shows the same trend. But its slope value is indicating an increase of 0.1492 as compared to 0.1893 of TROPOMI (see Fig. 7(a)). However, the monthly correlation of a MAX-DOAS with OMI and TROPOMI data not only improves R^2 significantly but also improves the slope. The slope with OMI data improved from 0.14 to 0.18 whereas, the slope of TROPOMI improved significantly from 0.18 to 0.40 as shown in Figs. 7(c) and 7(d) for OMI and TROPOMI respectively. The comparison of the slopes of OMI and TROPOMI vs. MAX-DOAS plots reveals that TROPOMI data is more synonymous to that of data obtained by MAX-DOAS. It can be attributed mainly owing to a higher and improved spatial and spectral resolution of TROPOMI than that of OMI. The slope of the correlation plots also exhibits underestimation of the satellite data and it is mainly due to restrictions of satellite sensors and retrieval algorithms. It can be further attributed to uncertainties caused by the coarse resolution of satellite sensors as compared to ground-based MAX-DOAS. Although satellite data underestimates the NO_2 column densities, it shows similar variation in NO_2 columns and can be speculated that there is a good agreement of MAX-DOAS measurements with TROPOMI data, instead of OMI.

Furthermore, the seasonal variations of NO_2 column densities for all three instruments are identical. As shown in Figs. 6(a) and 6(b) NO_2 column density peaks in the winter season while the lower NO_2 columns are observed in the monsoon season. Depending upon various factors i.e., OH concentration, photolysis rate and varying meteorological conditions, NO_2 has a lifetime of a few hours to about one day (Beirle *et al.*, 2003; Seinfeld and Pandis, 1997; Sheel *et al.*, 2010). The largest known sink of NO_x is a reaction of NO_2 with hydroxyl (OH) radical (Stavrakou *et al.*, 2013). As there is low temperature and limited solar flux is available during the winter season, there is less NO_2 loss due to reaction with OH radical that leads to higher NO_2 lifetime and column densities. The other contributing factor is fewer precipitation rates that hinder frequent OH production due to less availability of water vapors (Sheel *et al.*, 2010). This leads to relatively limited removal of NO_2 molecules. Furthermore, during the winter season increased usage of wood,

ORIGINAL RESEARCH
https://doi.org/10.4209/aaqr.210398

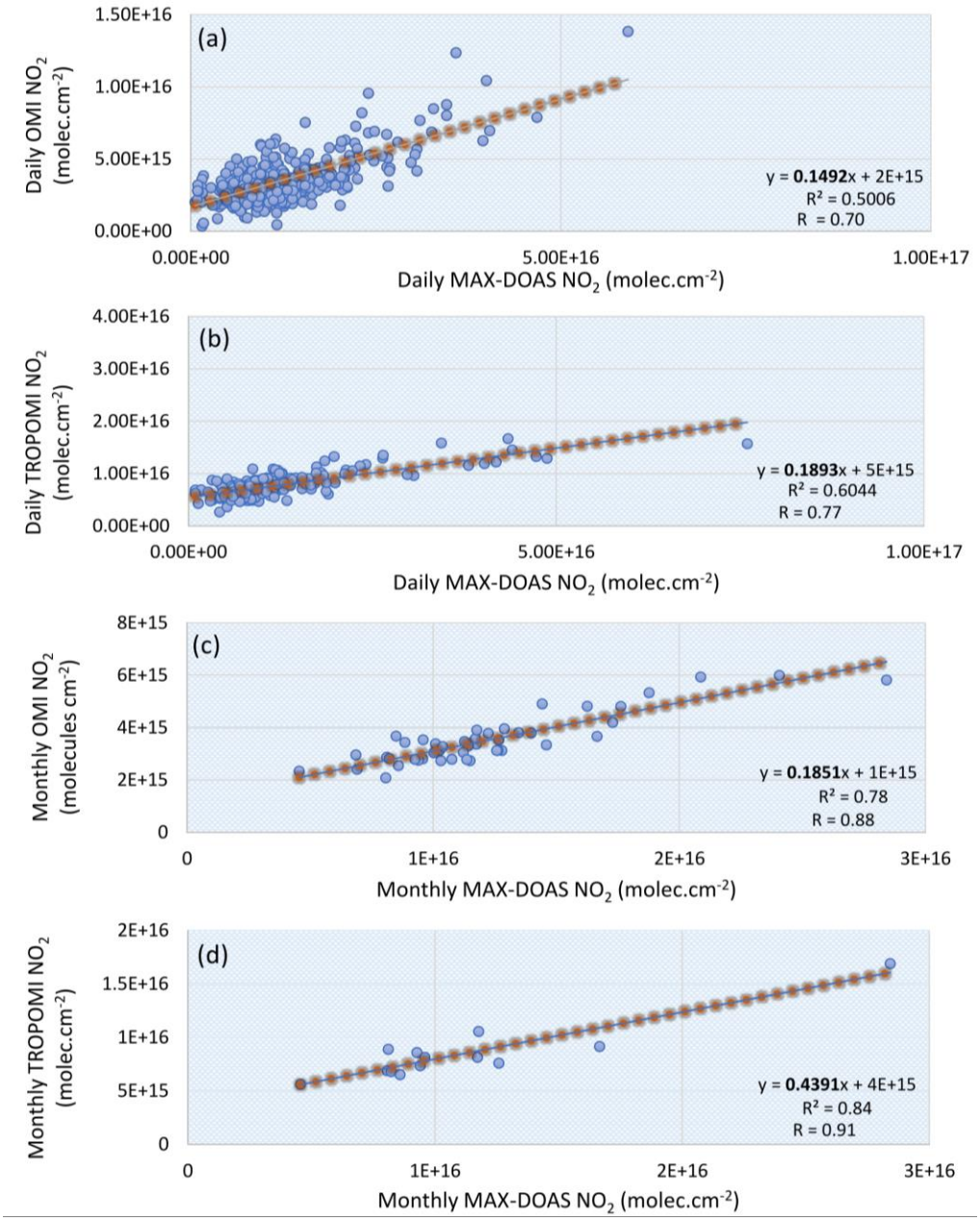

Fig. 7. Correlation plots between (a) daily MAX-DOAS NO_2 and OMI NO_2 (b) daily MAX-DOAS NO_2 and TROPOMI NO_2 (c) average monthly MAX-DOAS NO_2 (average of 1300–1400 h, UTC+5) and OMI NO_2 in molecules cm^{-2} from September 2015 to September 2019, and (d) average monthly MAX-DOAS NO_2 and TROPOMI NO_2 from September 2018 to September 2019.

cow dung and coal burning for cooking and space heating results in increased NO_2 emissions. Due to the longer NO_2 lifetime and more emissions of NO_2 during the winter season, higher NO_2 values are observed in winter season (Martin *et al.*, 2010). A similar trend can be observed in Fig. 6(b). Grey rectangles in Fig. 6(b) show the monsoon season in Pakistan and longer and heavier spells of monsoon rains. Therefore, the monsoon exhibits lower NO_2 columns in the seasonal cycle mainly due to the larger availability of OH radical causing a decreased NO_2 lifetime. This could also be attributed to the advection of moist clean air masses, heavy precipitation (wet scavenging) and strong actinic fluxes during the monsoon season (Wang and Jacob, 1998; Jacob, 2003; Khokhar *et al.*, 2015). The observations from satellite as well as ground-based instruments recorded the highest NO_2 column densities when days are longer than night and photolysis of NO_2 occurs for a much longer time.

Table 1. Error analysis computed over a different time duration under the study period.

Instruments	Duration	Time Period	Root Mean Square Error (RMSE)	Mean Absolute Error (MAE)	Mean Bias (MB)
MAX-DOAS vs. OMI	2015–2019	Daily	1.08E+16	8.82E+15	8.59E+15
		Monthly	9.46E+15	8.74E+15	8.74E+15
MAX-DOAS vs. OMI	2018–2019	Daily	8.87E+15	7.34E+15	7.24E+15
		Monthly	9.42E+15	8.09E+15	8.09E+15
MAX-DOAS vs. TROPOMI	2018–2019	Daily	4.49E+15	3.40E+15	2.15E+15
		Monthly	4.34E+15	3.04E+15	2.76E+15

4.1 Error Analysis

Error analysis between the MAX-DOAS measurements and satellite observations i.e., OMI and TROPOMI were performed by finding the root mean square error (RMSE) and the mean absolute error (MAE) given by Eqs. (8) and (9), respectively.

$$RMSE = \sqrt{\frac{1}{n}\sum_{i=1}^{n}\left(T_{(MAX-DOAS)_i} - T_{(SATELLITE)_i}\right)} \tag{8}$$

$$MAE = \frac{1}{n}\sum_{i=1}^{n}\left|T_{(MAX-DOAS)_i} - T_{(SATELLITE)_i}\right| \tag{9}$$

where n is the number of observations. Besides computing differences in averages, overestimation or underestimation of a model can be quantified by calculating the mean bias (MB), which is given by Eq. (10):

$$MB = \frac{1}{n}\sum_{i=1}^{n}\left(T_{(MAX-DOAS)_i} - T_{(SATELLITE)_i}\right) \tag{10}$$

Error analysis computed over a different time duration under the study period on daily as well as a monthly basis is presented in Table 1. The daily RMSE, MAE and MB between MAX-DOAS and OMI for the study period (2015–2019) were 1.08E+16, 8.82E+15 and 8.59E+15 respectively while on monthly basis these were 9.46E+15, 8.74E+15 and 8.74+15 respectively. The daily and monthly analysis of RMSE, MAE and MB for the period of 2018–2019 were also performed to check the synchronization of satellite observations (TROPOMI and OMI) with ground-based MAX-DOAS measurements. The daily RMSE, MAE and MB between MAX-DOAS and OMI for the period of 2018–2019 were 8.87E+15, 7.34E+15 and 7.24E+15 respectively while on monthly basis these were 9.42E+15, 8.09E+15 and 8.09+15 respectively. Similarly, the daily RMSE, MAE and MB between MAX-DOAS and TROPOMI for the period of 2018-2019 were 4.49E+15, 3.40E+15 and 2.15E+15 respectively while on monthly basis these were 4.34E+15, 3.04E+15 and 2.76E+15 respectively. These error analysis of MAX-DOAS vs. OMI and TROPOMI on a daily as well as monthly basis indicates that TROPOMI measurements are more synchronized with ground-based MAX-DOAS measurements. It is pertinent to note that TROPOMI's finer spatial resolution has significantly improved the biases.

5 CONCLUSIONS

- Different NO_2 retrieval settings found in the literature were compared with the settings used in this study for 01 November 2017. Correlation plots showed good agreement among the measurements with the least $R^2 = 0.972$ ($r = 0.98$).
- For validation of the observations, ground-based observations were compared with OMI and TROPOMI satellite data which showed similar trends, but underestimation of results is

observed for both satellite-based observations. MAX-DOAS measurements have shown a strong positive correlation with both OMI and TROPOMI observations.

- The correlation for daily measurements between MAX-DOAS vs. OMI and TROPMI has shown a very good positive correlation. The monthly correlation (R^2) of MAX-DOAS vs. OMI and TROPOMI is 0.883 and 0.919 respectively. The value of slope for daily data has shown that for every increase in MAX-DOAS value by 1, there is increase of 0.1893 and 0.1492 for TROPMI and OMI respectively. However, for average monthly values slope is 0.40 and 0.18 for TROPOMI and OMI receptively.
- The error analysis of MAX-DOAS vs. OMI and TROPOMI on a daily as well as monthly basis indicates that TROPOMI measurements are more synchronized with ground-based MAX-DOAS measurements. There is a good level of agreement between MAX-DOAS and TROPOMI as compared to MAX-DOAS and OMI. It is important to note that TROPOMI's resolution is significantly finer than OMI's due to which there is more biasness for OMI values. Based on these results, it is pertinent to mention that owing to its high spatial resolution, TROPOMI measurements are able to capture the local NO_2 pollution much better than OMI and its predecessor instruments like GOME-2, SCIAMACHY, GOME. Furthermore, the seasonal trends of NO_2 for all three instruments have shown maximum NO_2 values during winter while the minimum for the monsoon season.

ACKNOWLEDGMENTS

We acknowledge the free use of Tropospheric NO_2 column data from the TROPOMI and OMI sensors. We acknowledge NUST Islamabad, Pakistan for providing partial financial support as a Master thesis research fund to conduct this study. Very special gratitude goes to the satellite group of Max-Planck Institute for Chemistry Mainz, Germany for providing the mini MAX-DOAS instrument.

DATA ACCESS

Data described in this manuscript is available at https://doi.org/10.5281/zenodo.5495812

REFERENCES

Ali, M., Athar, M. (2008). Air pollution due to traffic, air quality monitoring along three sections of National Highway N-5, Pakistan. Environ. Monit. Assess. 136, 219–226. https://doi.org/10.1007/s10661-007-9677-3

Ali, S.M., Malik, F., Anjum, M.S., Siddiqui, G.F., Anwar, M.N., Lam, S.S., Nizami, A.S., Khokhar, M.F. (2021). Exploring the linkage between $PM_{2.5}$ levels and COVID-19 spread and its implications for socio-economic circles. Environ. Res. 193, 110421. https://doi.org/10.1016/j.envres.2020.110421

Anjum, M.S., Ali, S.M., Subhani, M.A., Anwar, M.N., Nizami, A.S., Ashraf, U., Khokhar, M.F. (2021). An emerged challenge of air pollution and ever-increasing particulate matter in Pakistan; A critical review. J. Hazard. Mater. 402, 123943. https://doi.org/10.1016/j.jhazmat.2020.123943

Anwar, M.N., Shabbir, M., Tahir, E., Iftikhar, M., Saif, H., Tahir, A., Murtaza, M.A., Khokhar, M.F., Rehan, M., Aghbashlo, M., Tabatabaei, M., Nizami, A.S. (2021). Emerging challenges of air pollution and particulate matter in China, India, and Pakistan and mitigating solutions. J. Hazard. Mater. 416, 125851. https://doi.org/10.1016/j.jhazmat.2021.125851

Athanasopoulou, E., Tombrou, M., Pandis, S.N., Russell, A.G. (2008). The role of sea-salt emissions and heterogeneous chemistry in the air quality of polluted coastal areas. Atmos. Chem. Phys. 8, 5755–5769. https://doi.org/10.5194/acp-8-5755-2008

Beirle, S., Platt, U., Wenig, M., Wagner, T. (2003). Weekly cycle of NO_2 by GOME measurements: A signature of anthropogenic sources. Atmos. Chem. Phys. 3, 2225–2232. https://doi.org/10.5194/acp-3-2225-2003

Bilal, M., Mhawish, A., Nichol, J.E., Qiu, Z., Nazeer, M., Ali, M.A., de Leeuw, G., Levy, R.C., Wang, Y., Chen, Y. (2021). Air pollution scenario over Pakistan: Characterization and ranking of

extremely polluted cities using long-term concentrations of aerosols and trace gases. Remote Sens. Environ. 264, 112617. https://doi.org/10.1016/j.rse.2021.112617

Bobrowski, N., Hönninger, G., Galle, B., Platt, U.J.N. (2003). Detection of bromine monoxide in a volcanic plume. Nature 423, 273. https://doi.org/10.1038/nature01625

Boersma, K., Eskes, H., Dirksen, R., Van Der A, R., Veefkind, J., Stammes, P., Huijnen, V., Kleipool, Q., Sneep, M., Claas, J. (2011). An improved tropospheric NO_2 column retrieval algorithm for the Ozone Monitoring Instrument. Atmos. Meas. Tech. 4, 1905–1928. https://doi.org/10.5194/amt-4-1905-2011

Burkholder, J.B., Talukdar, R.K. (1994). Temperature dependence of the ozone absorption spectrum over the wavelength range 410 to 760 nm. J. Geophys. Res. 21, 581–584. https://doi.org/10.1029/93GL02311

Chan, K.L., Hartl, A., Lam, Y.F., Xie, P.H., Liu, W.Q., Cheung, H.M., Lampel, J., Pöhler, D., Li, A., Xu, J., Zhou, H.J., Ning, Z., Wenig, M.O. (2015). Observations of tropospheric NO_2 using ground based MAX-DOAS and OMI measurements during the Shanghai World Expo 2010. Atmos. Environ. 119, 45–58. https://doi.org/10.1016/j.atmosenv.2015.08.041

Chan, K. (2017). Biomass burning sources and their contributions to the local air quality in Hong Kong. Sci. Total Environ. 596, 212–221. https://doi.org/10.1016/j.scitotenv.2017.04.091

Chan, K.L., Wiegner, M., Wenig, M., Pöhler, D. (2018). Observations of tropospheric aerosols and NO_2 in Hong Kong over 5 years using ground based MAX-DOAS. Sci. Total Environ. 619–620, 1545–1556. https://doi.org/10.1016/j.scitotenv.2017.10.153

Chan, K.L., Wang, Z., Ding, A., Heue, K.P., Shen, Y., Wang, J., Zhang, F., Shi, Y., Hao, N., Wenig, M. (2019). MAX-DOAS measurements of tropospheric NO_2 and HCHO in Nanjing and a comparison to ozone monitoring instrument observations. Atmos. Chem. Phys. 19, 10051–10071. https://doi.org/10.5194/acp-19-10051-2019

Chan, K.L., Wiegner, M., van Geffen, J., De Smedt, I., Alberti, C., Cheng, Z., Ye, S., Wenig, M. (2020). MAX-DOAS measurements of tropospheric NO_2 and HCHO in Munich and the comparison to OMI and TROPOMI satellite observations. Atmos. Meas. Tech. 13, 4499–4520. https://doi.org/10.5194/amt-13-4499-2020

Cheng, S., Ma, J., Cheng, W., Yan, P., Zhou, H., Zhou, L., Yang, P. (2019). Tropospheric NO_2 vertical column densities retrieved from ground-based MAX-DOAS measurements at Shangdianzi regional atmospheric background station in China. J. Environ. Sci. 80, 186–196. https://doi.org/10.1016/j.jes.2018.12.012

Coburn, S., Dix, B., Sinreich, R., Volkamer, R. (2011). The CU ground MAX-DOAS instrument: Characterization of RMS noise limitations and first measurements near Pensacola, FL of BrO, IO, and CHOCHO. Atmos. Meas. Tech. 4, 2421–2439. https://doi.org/10.5194/amt-4-2421-2011

Crutzen, P.J. (1970). The influence of nitrogen oxides on the atmospheric ozone content. Q. J. R. Meteorolog. Soc. 96, 320–325. https://doi.org/10.1002/qj.49709640815

Dimitropoulou, E., Hendrick, F., Pinardi, G., Friedrich, M.M., Merlaud, A., Tack, F., De Longueville, H., Fayt, C., Hermans, C., Laffineur, Q. (2020). Validation of TROPOMI tropospheric NO_2 columns using dual-scan multi-axis differential optical absorption spectroscopy (MAX-DOAS) measurements in Uccle, Brussels. Atmos. Meas. Tech. 13, 5165–5191. https://doi.org/10.5194/amt-13-5165-2020

Dix, B., Koenig, T.K., Volkamer, R. (2016). Parameterization retrieval of trace gas volume mixing ratios from Airborne MAX-DOAS. Atmos. Meas. Tech. 9, 5655–5675. https://doi.org/10.5194/amt-9-5655-2016

Drosoglou, T., Koukouli, M.E., Kouremeti, N., Bais, A.F., Zyrichidou, I., Balis, D., van der A, R.J., Xu, J., Li, A. (2018). MAX-DOAS NO_2 observations over Guangzhou, China; ground-based and satellite comparisons. Atmos. Meas. Tech. 11, 2239–2255. https://doi.org/10.5194/amt-11-2239-2018

U.S. Environmental Protection Agency (U.S. EPA) (2006). Air Quality Criteria for Ozone and Related Photochemical Oxidants (Final Report, 2006). U.S. Environmental Protection Agency, Washington, DC, EPA/600/R-05/004aF-cF.

Franco, B., Hendrick, F., Van Roozendael, M., Müller, J.F., Stavrakou, T., Marais, E.A., Bovy, B., Bader, W., Fayt, C., Hermans, C., Lejeune, B., Pinardi, G., Servais, C., Mahieu, E. (2015). Retrievals of formaldehyde from ground-based FTIR and MAX-DOAS observations at the Jungfraujoch station and comparisons with GEOS-Chem and IMAGES model simulations. Atmos. Meas. Tech.

8, 1733–1756. https://doi.org/10.5194/amt-8-1733-2015

Gratsea, M., Vrekoussis, M., Richter, A., Wittrock, F., Schönhardt, A., Burrows, J., Kazadzis, S., Mihalopoulos, N., Gerasopoulos, E. (2016). Slant column MAX-DOAS measurements of nitrogen dioxide, formaldehyde, glyoxal and oxygen dimer in the urban environment of Athens. Atmos. Environ. 135, 118–131. https://doi.org/10.1016/j.atmosenv.2016.03.048

Halla, J.D., Wagner, T., Beirle, S., Brook, J.R., Hayden, K.L., O'Brien, J.M., Ng, A., Majonis, D., Wenig, M.O., McLaren, R. (2011). Determination of tropospheric vertical columns of NO_2 and aerosol optical properties in a rural setting using MAX-DOAS. Atmos. Chem. Phys. 11, 12475–12498. https://doi.org/10.5194/acp-11-12475-2011

Hendrick, F., Müller, J.F., Clémer, K., Wang, P., De Mazière, M., Fayt, C., Gielen, C., Hermans, C., Ma, J.Z., Pinardi, G., Stavrakou, T., Vlemmix, T., Van Roozendael, M. (2014). Four years of ground-based MAX-DOAS observations of HONO and NO_2 in the Beijing area. Atmos. Chem. Phys. 14, 765–781. https://doi.org/10.5194/acp-14-765-2014

Hermans, C. (2011). BIRA-IASB Spectroscopy Lab. http://spectrolab.aeronomie.be/index.htm (accessed 27 October 2020).

Hönninger, G., von Friedeburg, C., Platt, U. (2004). Multi axis differential optical absorption spectroscopy (MAX-DOAS). Atmos. Chem. Phys. 4, 231–254. https://doi.org/10.5194/acp-4-231-2004

Jacob, D.J. (2003). The Oxidizing Power of the Atmosphere. in: Handbook of Weather, Climate and Water: Atmospheric Chemistry, Hydrology, and Societal Impacts, Potter, T.D., Colman, B.R. (Eds.), pp. 29–46, John Wiley, Hoboken, N. J.

Javed, Z., Liu, C., Khokhar, M., Tan, W., Liu, H., Xing, C., Ji, X., Tanvir, A., Hong, Q., Sandhu, O., Rehman, A. (2019a). Ground-based MAX-DOAS observations of CHOCHO and HCHO in Beijing and Baoding, China. Remote Sens. 11, 1524. https://doi.org/10.3390/rs11131524

Javed, Z., Liu, C., Khokhar, M.F., Xing, C., Tan, W., Subhani, M.A., Rehman, A., Tanvir, A. (2019a). Investigating the impact of Glyoxal retrieval from MAX-DOAS observations during haze and non-haze conditions in Beijing. J. Environ. Sci. 80, 296–305. https://doi.org/10.1016/j.jes.2019.01.008

Khan, W.A., Khokhar, M.F., Shoaib, A., Nawaz, R. (2018). Monitoring and analysis of formaldehyde columns over Rawalpindi-Islamabad, Pakistan using MAX-DOAS and satellite observation. Atmos. Pollut. Res. 9, 840–848. https://doi.org/10.1016/j.apr.2017.12.008

Khokhar, M.F., Yasmin, N., Fatima, N., Beirle, S., Wagner, T. (2015). Detection of trends and seasonal variation in tropospheric nitrogen dioxide over Pakistan. Aerosol Air Qual. Res. 15, 2508–2524. https://doi.org/10.4209/aaqr.2015.03.0157

Khokhar, M., Naveed, S., Butt, J., Abbas, Z.J.A. (2016a). Comparative analysis of atmospheric glyoxal column densities retrieved from MAX-DOAS observations in Pakistan and during MAD-CAT field campaign in Mainz, Germany. Atmosphere 7, 68. https://doi.org/10.3390/atmos7050068

Khokhar, M.F., Mehdi, H., Abbas, Z., Javed, Z. (2016b). Temporal assessment of NO_2 pollution levels in urban centers of Pakistan by employing ground-based and satellite observations. Aerosol Air Qual. Res. 16, 1854–1867. https://doi.org/10.4209/aaqr.2015.08.0518

Khokhar, M.F., Nisar, M., Noreen, A., Khan, W.R., Hakeem, K.R. (2017). Investigating the nitrogen dioxide concentrations in the boundary layer by using multi-axis spectroscopic measurements and comparison with satellite observations. Environ. Sci. Pollut. Res. 24, 2827–2839. https://doi.org/10.1007/s11356-016-7907-3

Khokhar, M.F., Anjum, M.S., Salam, A., Sinha, V., Naja, M., Tanimoto, H., Crawford, J.H., Mead, M.I. (2021). Countries of the Indo-Gangetic Plain must unite against air pollution. Nature 598, 415–415. https://doi.org/10.1038/d41586-021-02829-4

Kreher, K., Van Roozendael, M., Hendrick, F., Apituley, A., Dimitropoulou, E., Frieß, U., Richter, A., Wagner, T., Abuhassan, N., Ang, L. (2019). Intercomparison of NO_2, O_4, O_3 and HCHO slant column measurements by MAX-DOAS and zenith-sky UV-Visible spectrometers during the CINDI-2 campaign. Atmos. Meas. Tech. https://doi.org/10.5194/amt-13-2169-2020

Kreher, K., Van Roozendael, M., Hendrick, F., Apituley, A., Dimitropoulou, E., Frieß, U., Richter, A., Wagner, T., Lampel, J., Abuhassan, N., Ang, L., Anguas, M., Bais, A., Benavent, N., Bösch, T., Bognar, K., Borovski, A., Bruchkouski, I., Cede, A., Chan, K.L., *et al.* (2020). Intercomparison of NO_2, O_4, O_3 and HCHO slant column measurements by MAX-DOAS and zenith-sky UV–visible

spectrometers during CINDI-2. Atmos. Meas. Tech. 13, 2169–2208. https://doi.org/10.5194/amt-13-2169-2020

Lee, H., Kim, Y.J., Jung, J., Lee, C., Heue, K.P., Platt, U., Hu, M., Zhu, T. (2009). Spatial and temporal variations in NO_2 distributions over Beijing, China measured by imaging differential optical absorption spectroscopy. J. Environ. Manage. 90, 1814–1823. https://doi.org/10.1016/j.jenvman.2008.11.025

Leser, H., Hönninger, G., Platt, U. (2003). MAX-DOAS measurements of BrO and NO_2 in the marine boundary layer. Geophys. Res. Lett. 30, 1537. https://doi.org/10.1029/2002GL015811

Lin, J.T., Martin, R.V., Boersma, K.F., Sneep, M., Stammes, P., Spurr, R., Wang, P., Van Roozendael, M., Clémer, K., Irie, H. (2014). Retrieving tropospheric nitrogen dioxide from the Ozone Monitoring Instrument: Effects of aerosols, surface reflectance anisotropy, and vertical profile of nitrogen dioxide. Atmos. Chem. Phys. 14, 1441–1461. https://doi.org/10.5194/acp-14-1441-2014

Liu, Q., Ma, T., Olson, M.R., Liu, Y., Zhang, T., Wu, Y., Schauer, J.J. (2016). Temporal variations of black carbon during haze and non-haze days in Beijing. Sci. Rep. 6, 33331. https://doi.org/10.1038/srep33331

Lohberger, F., Hönninger, G., Platt, U. (2004). Ground-based imaging differential optical absorption spectroscopy of atmospheric gases. Appl. Opt. 43, 4711. https://doi.org/10.1364/AO.43.004711

Ma, J.Z., Beirle, S., Jin, J.L., Shaiganfar, R., Yan, P., Wagner, T. (2013). Tropospheric NO_2 vertical column densities over Beijing: Results of the first three years of ground-based MAX-DOAS measurements (2008–2011) and satellite validation. Atmos. Chem. Phys. 13, 1547–1567. https://doi.org/10.5194/acp-13-1547-2013

Majewski, G., Czechowski, P.O., Badyda, A., Brandyk, A. (2014). Effect of air pollution on visibility in urban conditions. Warsaw case study. Environ. Prot. Eng. 40, 47–64. https://doi.org/10.37190/epe140204

Malik, A., Hussain, E., Baig, S., Khokhar, M.F. (2020). Forecasting CO_2 emissions from energy consumption in Pakistan under different scenarios: The China–Pakistan economic corridor. Greenhouse Gases Sci. Technol. 10, 380–389. https://doi.org/10.1002/ghg.1968

Martin, P., Cabañas, B., Villanueva, F., Gallego, M.P., Colmenar, I., Salgado, S. (2010). Ozone and nitrogen dioxide levels monitored in an urban area (Ciudad Real) in central-southern Spain. Water Air Soil Pollut. 208, 305–316. https://doi.org/10.1007/s11270-009-0168-8

Müller, J., Kharbouche, S., Gobron, N., Scanlon, T., Govaerts, Y., Danne, O., Schultz, J., Lattanzio, A., Peters, E., De Smedt, I. (2016). Recommendations (scientific) on best practices for retrievals for Land and Atmosphere ECVs (QA4ECV Deliverable 4.2 version 1.0), 186 pp. D4.

Naheed, G., Kazmi, D.H., Rasul, G. (2013). Seasonal variation of rainy days in Pakistan. Pakistan J. Meteorol. 9, 9–13.

Peters, E., Wittrock, F., Großmann, K., Frieß, U., Richter, A., Burrows, J.P. (2012). Formaldehyde and nitrogen dioxide over the remote western Pacific Ocean: SCIAMACHY and GOME-2 validation using ship-based MAX-DOAS observations. Atmos. Chem. Phys. 12, 11179–11197. https://doi.org/10.5194/acp-12-11179-2012

Platt, U., Stutz, J. (2008). Differential Optical Absorption Spectroscopy Principles and Applications, Differential Optical Absorption Spectroscopy. Springer, pp. 135–174. https://doi.org/10.1007/978-3-540-75776-4_6

Rothman, L.S. (2010). The evolution and impact of the HITRAN molecular spectroscopic database. J. Quant. Spectrosc. Radiat. Transfer 111, 1565–1567. https://doi.org/10.1016/j.jqsrt.2010.01.027

Schenkeveld, V., Jaross, G., Marchenko, S., Haffner, D., Kleipool, Q.L., Rozemeijer, N.C., Veefkind, J.P., Levelt, P.F. (2017). In-flight performance of the ozone monitoring instrument. Atmos. Meas. Tech. 10, 1957–1986. https://doi.org/10.5194/amt-10-1957-2017

Seinfeld, J.H., Pandis, S.N. (1997). Atmospheric chemistry and physics: From air pollution to climate change. Wiley-Interscience, New York.

Serdyuchenko, A., Gorshelev, V., Weber, M., Chehade, W., Burrows, J.P. (2014). High spectral resolution ozone absorption cross-sections – Part 2: Temperature dependence. Atmos. Meas. Tech. 7, 625–636. https://doi.org/10.5194/amt-7-625-2014

Shabbir, Y., Khokhar, M.F., Shaiganfar, R., Wagner, T. (2016). Spatial variance and assessment of nitrogen dioxide pollution in major cities of Pakistan along N5-Highway. J. Environ. Sci. 43, 4–14. https://doi.org/10.1016/j.jes.2015.04.038

Shaiganfar, R., Beirle, S., Sharma, M., Chauhan, A., Singh, R.P., Wagner, T. (2011). Estimation of NO_x emissions from Delhi using Car MAX-DOAS observations and comparison with OMI satellite data. Atmos. Chem. Phys. 11, 10871–10887. https://doi.org/10.5194/acp-11-10871-2011

Shaiganfar, R., Beirle, S., Petetin, H., Zhang, Q., Beekmann, M., Wagner, T. (2015). New concepts for the comparison of tropospheric NO_2 column densities derived from car-MAX-DOAS observations, OMI satellite observations and the regional model CHIMERE during two MEGAPOLI campaigns in Paris 2009/10. Atmos. Meas. Tech. 8, 2827–2852. https://doi.org/10.5194/amt-8-2827-2015

Sheel, V., Lal, S., Richter, A., Burrows, J. P. (2010). Comparison of satellite observed tropospheric NO_2 over India with model simulations. Atmos. Environ. 44, 3314–3321. https://doi.org/10.1016/j.atmosenv.2010.05.043

Soto-Martinez, M., Sly, P.D. (2010). Review Series: What goes around, comes around: childhood influences on later lung health?: Relationship between environmental exposures in children and adult lung disease: The case for outdoor exposures. Chron. Respir. Dis. 7, 173–186. https://doi.org/10.1177/1479972309345929

Stavrakou, T., Müller, J.F., Boersma, K.F., Van Der A, R.J., Kurokawa, J., Ohara, T., Zhang, Q. (2013). Key chemical NO_x sink uncertainties and how they influence top-down emissions of nitrogen oxides. Atmos. Chem. Phys. 13, 9057–9082. https://doi.org/10.5194/acp-13-9057-2013

Tack, F., Hendrick, F., Goutail, F., Fayt, C., Merlaud, A., Pinardi, G., Hermans, C., Pommereau, J.-P., Van Roozendael, M. (2015). Tropospheric nitrogen dioxide column retrieval from ground-based zenith–sky DOAS observations. Atmos. Meas. Tech. 8, 2417–2435. https://doi.org/10.5194/amt-8-2417-2015

Tariq, S., Ali, M., Mahmood, K., Batool, S.A., Rana, A.D. (2014). A study of tropospheric NO_2 variability over Pakistan using OMI data. Atmos. Pollut. Res. 5, 709–720. https://doi.org/10.5094/APR.2014.080

Thalman, R., Volkamer, R. (2013). Temperature dependent absorption cross-sections of O_2–O_2 collision pairs between 340 and 630 nm and at atmospherically relevant pressure. Phys. Chem. Chem. Phys. 15, 15371. https://doi.org/10.1039/c3cp50968k

Tian, X., Xie, P., Xu, J., Li, A., Wang, Y., Qin, M., Hu, Z. (2018). Long-term observations of tropospheric NO_2, SO_2 and HCHO by MAX-DOAS in Yangtze River Delta area, China. J. Environ. Sci. 71, 207–221. https://doi.org/10.1016/j.jes.2018.03.006

Trasande, L., Thurston, G.D. (2005). The role of air pollution in asthma and other pediatric morbidities. J. Allergy Clin. Immunol. 115, 689–699. https://doi.org/10.1016/j.jaci.2005.01.056

Valavanidis, A., Fiotakis, K., Vlachogianni, T. (2008). Airborne particulate matter and human health: Toxicological assessment and importance of size and composition of particles for oxidative damage and carcinogenic mechanisms. J. Environ. Sci. Health., Part C 26, 339–362. https://doi.org/10.1080/10590500802494538

Van Geffen, J., Boersma, K.F., Eskes, H., Sneep, M., Ter Linden, M., Zara, M., Veefkind, J.P. (2020). S5P TROPOMI NO_2 slant column retrieval: Method, stability, uncertainties and comparisons with OMI. Atmos. Meas. Tech. 13, 1315–1335. https://doi.org/10.5194/amt-13-1315-2020

Vandaele, A.C., Hermans, C., Simon, P.C., Van Roozendael, M., Guilmot, J.M., Carleer, M., Colin, R. (1996). Fourier transform measurement of NO_2 absorption cross-section in the visible range at room temperature. J. Atmos. Chem. 25, 289–305. https://doi.org/10.1007/BF00053797

Vlemmix, T., Hendrick, F., Pinardi, G., De Smedt, I., Fayt, C., Hermans, C., Piters, A., Wang, P., Levelt, P., Van Roozendael, M. (2015). MAX-DOAS observations of aerosols, formaldehyde and nitrogen dioxide in the Beijing area: Comparison of two profile retrieval approaches. Atmos. Meas. Tech. 8, 941–963. https://doi.org/10.5194/amt-8-941-2015

Wagner, T., Ibrahim, O., Shaiganfar, R., Platt, U. (2010). Mobile MAX-DOAS observations of tropospheric trace gases. Atmos. Meas. Tech. 3, 129–140. https://doi.org/10.5194/amt-3-129-2010

Wang, S., Zhou, B., Wang, Z., Yang, S., Hao, N., Valks, P., Trautmann, T., Chen, L. (2012). Remote sensing of NO_2 emission from the central urban area of Shanghai (China) using the mobile DOAS technique. J. Geophys. Res. 117, D13305. https://doi.org/10.1029/2011JD016983

Wang, T., Hendrick, F., Wang, P., Tang, G., Clémer, K., Yu, H., Fayt, C., Hermans, C., Gielen, C., Müller, J.F. (2014). Evaluation of tropospheric SO_2 retrieved from MAX-DOAS measurements in Xianghe, China. Atmos. Chem. Phys. 14, 11149–11164. https://doi.org/10.5194/acp-14-11149-2014

Wang, Y., Jacob, D.J. (1998). Anthropogenic forcing on tropospheric ozone and OH since preindustrial times. J. Geophys. Res. 103, 31123–31135. https://doi.org/10.1029/1998JD100004

Wang, Y., Lampel, J., Xie, P., Beirle, S., Li, A., Wu, D., Wagner, T. (2017). Ground-based MAX-DOAS observations of tropospheric aerosols, NO_2, SO_2 and HCHO in Wuxi, China, from 2011 to 2014. Atmos. Chem. Phys. 17, 2189–2215. https://doi.org/10.5194/acp-17-2189-2017

World Health Organization (WHO) (2006). WHO Air quality guidelines for particulate matter, ozone, nitrogen dioxide and sulfur dioxide: global update 2005: summary of risk assessment. World Health Organization. https://apps.who.int/iris/handle/10665/69477

Wittrock, F., Oetjen, H., Richter, A., Fietkau, S., Medeke, T., Rozanov, A., Burrows, J.P. (2004). MAX-DOAS measurements of atmospheric trace gases in Ny-Ålesund - Radiative transfer studies and their application. Atmos. Chem. Phys. 4, 955–966. https://doi.org/10.5194/acp-4-955-2004

Yang, T., Si, F., Luo, Y., Zhan, K., Wang, P., Zhou, H., Zhao, M., Liu, W. (2019). Source contribution analysis of tropospheric NO_2 based on two-dimensional MAX-DOAS measurements. Atmos. Environ. 210, 186–197. https://doi.org/10.1016/j.atmosenv.2019.04.058

Youssef Agha, A.H., Jayawardene, W.P., Lohrmann, D.K., El Afandi, G.S. (2012). Air pollution indicators predict outbreaks of asthma exacerbations among elementary school children: Integration of daily environmental and school health surveillance systems in Pennsylvania. J. Environ. Monit. 14, 3202. https://doi.org/10.1039/c2em30430a

Zara, M., Boersma, K.F., De Smedt, I., Richter, A., Peters, E., Van Geffen, J.H., Beirle, S., Wagner, T., Van Roozendael, M., Marchenko, S. (2018). Improved slant column density retrieval of nitrogen dioxide and formaldehyde for OMI and GOME-2A from QA4ECV: Intercomparison, uncertainty characterisation, and trends. Atmos. Meas. Tech. 11, 4033–4058. https://doi.org/10.5194/amt-11-4033-2018

Zeb, N., Khokhar, M.F., Pozzer, A., Khan, S.A. (2019). Exploring the temporal trends and seasonal behaviour of tropospheric trace gases over Pakistan by exploiting satellite observations. Atmos. Environ. 198, 279–290. https://doi.org/10.1016/j.atmosenv.2018.10.053